Surface accuracy and roughness parameters in free form grinding with the use of an spherical diamond head

Dokładność i chropowatość powierzchni po pięcioosiowym szlifowaniu ściernicą kulistą

JAN BUREK
ARTUR SZAJNA
JOANNA LISOWICZ
TOMASZ RYDZAK*

DOI: https://doi.org/10.17814/mechanik.2017.8-9.110

The article presents the results of experimental research for free form grinding of corundum ceramic with the use of an spherical diamond head. Article shows the influence of cutting depth and feed on roughness parameters and surface accuracy.
KEYWORDS: grinding, corundum ceramics, surface accuracy reproduction, spherical head diamond mounted points grinding tool

Due to the properties of ceramic materials, their abrasive treatment is technologically difficult. This applies particularly to the grinding of complex surfaces in which the treatment is most often used mounted wheels with diamond coating [1-3]. This process requires the use of multi-axis grinders equipped with high-speed spindles and precise axle positioning systems – only under this condition it is possible to grind elements of complex shapes made of ceramic or super-hard materials [4].

Ceramic materials are widely used in the art, and in medical engineering – especially aluminum oxide and zirconium are used for bone implants and dental [4, 5]. Such elements are made using small tools, which causes the cutting speed v_c to be within the range of 5÷10 m/s (in the case of grinding with conventional grinding wheels, it is 30÷45 m/s). For example: for a cutting speed of d_s = 5 mm to 10 m/s, the spindle speed of the machine should be at least n_s = 40,000 rpm.

In addition, in grinding with spherical grinding wheels, it is important to set the axis of the grinding wheel relative to the surface to be machined – to achieve the required effective cutting speed (fig. 1).

Depending on the angles of lead α and tilt β, the minimum and maximum effective cutting speeds take different values.

If α = 0° and β = 0° (spindle axis perpendicular to the surface), then the cutting speeds take the following values:

$$v_{c\,min} = \frac{\pi \cdot n_s \cdot 2 \cdot \sqrt{\left(\frac{1}{2}d_s\right)^2 - \left(\frac{1}{2}d_s - a_p\right)^2}}{60\,000}\ [m/s]$$

$$v_{c\,max} = \frac{\pi \cdot n_s \cdot d_s}{60\,000}\ [m/s]$$

where: a_p is the grinding depth.

* Dr hab. inż. Jan Burek prof. PRz (jburek@prz.edu.pl), mgr inż. Artur Szajna (a.szajna@prz.edu.pl), mgr inż. Joanna Lisowicz (j.lisowicz@prz.edu.pl), mgr inż. Tomasz Rydzak (t.rydzak@prz.edu.pl) – Katedra Technik Wytwarzania i Automatyzacji, Wydział Budowy Maszyn i Lotnictwa Politechniki Rzeszowskiej

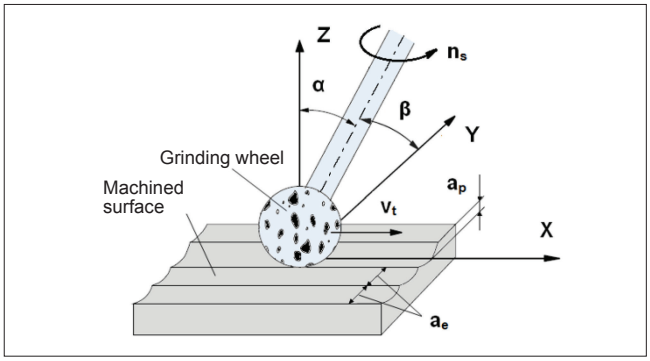

Fig. 1. Adjustment of grinding wheel axis (a_p – grinding depth, a_e – grinding width, α – lead angle, β – tilt angle, n_s – wheel speed)

If one of the angles (α or β) is different from zero, the cutting speeds are determined by the equations:

$$v_{c\,min} = \frac{\pi \cdot d_{s\,min} \cdot n_s}{60\,000}\ [m/s]$$

$$v_{c\,max} = \frac{\pi \cdot d_{s\,max} \cdot n_s}{60\,000}\ [m/s]$$

where:

$$d_{s\,min} = d_s \cdot \sin\left(\beta - \arccos\left(\frac{\frac{1}{2}d_s - R_{th}}{\frac{1}{2}d_s}\right)\right)\ [mm]$$

$$d_{s\,max} = d_s \cdot \sin\left(\beta + \arccos\left(\frac{\frac{1}{2}d_s - a_p}{\frac{1}{2}d_s}\right)\right)\ [mm]$$

while R_{th} is the theoretical height of the roughness (fig. 2).

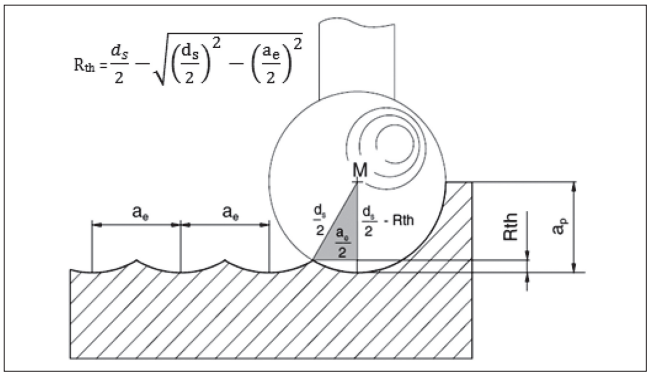

Fig. 2. Determination of maximum theoretical roughness R_{th} [4]

Test stand and the study

Grinding experiments were performed on the Ultrasonic 20 linear machining center of Sauer (fig. 3) equipped with the Sinumerik 840D control system. Dremel diamond

polishing wheels (7105), galvanized, with a diameter of d_s = 4.4 mm, were used. The workpiece was pre-cured alumina with an Al_2O_3 content of more than 98%.

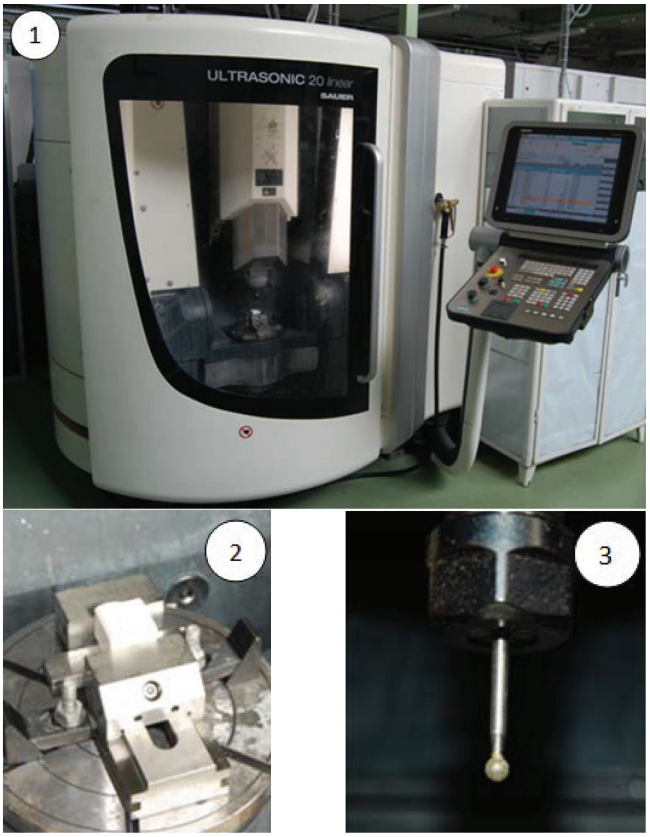

Fig. 3. Test stand: 1 – machine tool, 2 – working space with attached specimen, 3 – Dremel 7105 grinding wheel

Two identical specimens were prepared for the study, divided into three zones with a width of 10 mm (fig. 4). For each zone a different grinding allowance was calculated (Table). A new grinding wheel was used for the treatment of each sample.

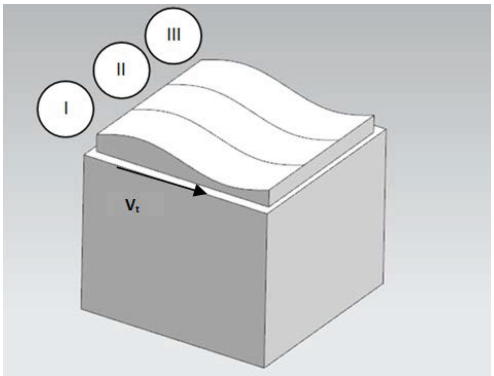

Fig. 4. Machined surface zones

The following parameters were used in the grinding process:

- cutting speed v_c = 5 m/s,
- tilt angle of of the wheel pin axis β = 40°,
- cutting depth a_p = 10 µm, 20 µm or 30 µm – depending on the treatment zone,
- cutting width a_e programmed so that the *Rt* value of the roughness does not exceed 1 µm.

The surface model for grinding and machining paths were generated using the NX9.0 program. The feed speed v_t was determined separately for each sample (200 mm/min for the first and 400 mm/min for the other).

Measurement of surface roughness and waveforms

Mahr MarSufr GD 120 profiler from Mahr, equipped with MFW-250: 1 (#6851855) measuring head, was used to measure surface roughness. Measurements of *Ra* and *Rz* parameters of surface roughness in the feed direction of the grinding wheel and perpendicular to feed were performed. Measurement of surface accuracy was performed on the Mahr XC 20 contour-graph. During the measurement, the nominal profile of the surface with the profile obtained after grinding with the parameters was compared. For the measurement deviation of the profile used PCV 350×58 mm 6033/1.

Ra and *Rz* roughness parameters measured in two mutually perpendicular directions obtained at different feed rates v_t are shown in figs. 5-8.

The surface roughness measurements obtained show that the *Ra* parameter measured in the direction of travel depends more on the feedrate than on the depth of the sanded material layer. Furthermore, the lowest *Ra* value was obtained during grinding with a_p = 30 µm depth.

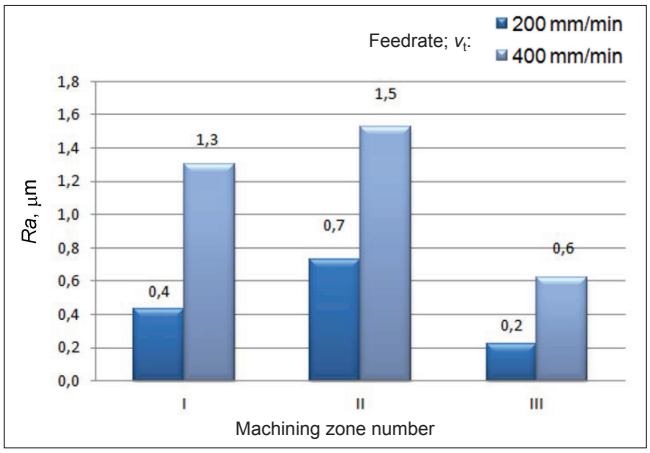

Fig. 5. *Ra* roughness parameter values obtained during the measurement in the direction corresponding to the feed direction

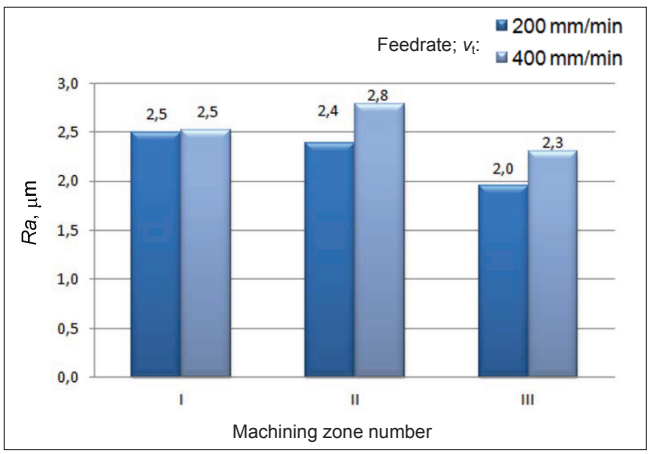

Fig. 6. *Ra* roughness parameter values obtained during measurement in a direction perpendicular to the feed direction

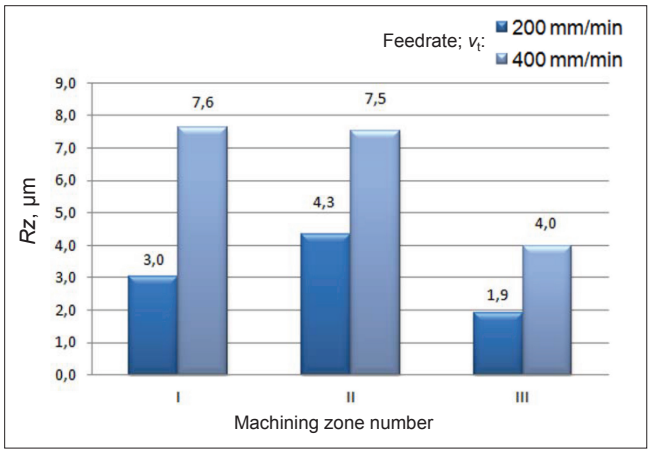

Fig. 7. Roughness *Rz* values obtained during the measurement in the direction corresponding to the feed direction

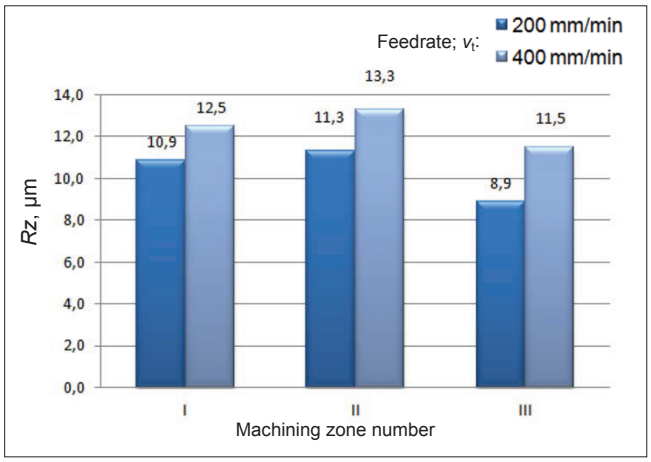

Fig. 8. Roughness *Rz* values obtained during the measurement in the direction perpendicular to the feed direction

In the opposite direction to the feedrate of the wheel, the *Ra* parameter is less dependent on the feed speed, and the impact of the cutting depth is less pronounced. The roughness coefficient *Rz* is decomposed in the same way. For both *Ra* and *Rz* parameters, the best results were obtained at feed rate v_t = 200 mm/min and cutting depth a_p = 30 µm.

Measurements of deviations of the shape along the contour of the measured surface of the sample are shown in figs. 9-11.

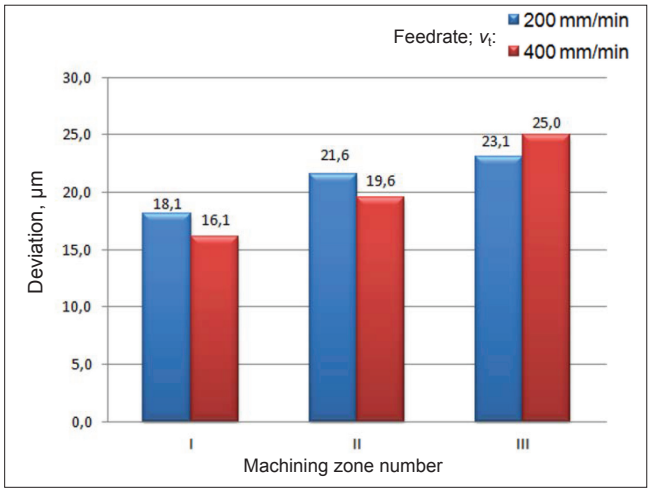

Fig. 9. Comparison of shape deviation values

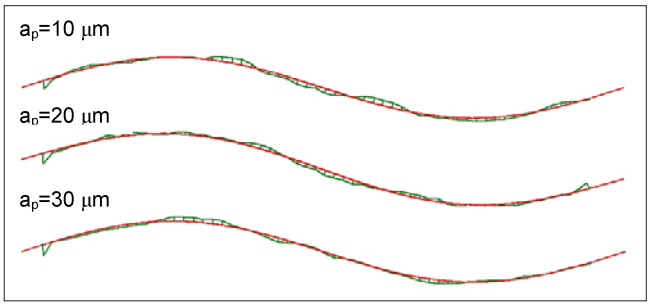

Fig. 10. Distribution of deviation of the shape of the actual profile (green color) determined in relation to the nominal profile (red color) for the feedrate of 200 mm/min

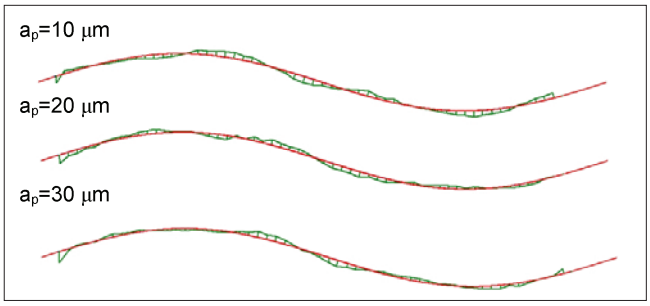

Fig. 11. Distribution of deviation of actual profile (green color) determined in relation to nominal profile (red color) for feedrate 400 mm/min

The profile deviations shown in the diagrams show that less grinding is achieved when grinding with a lower feed speed in the area of the concave surface than with a higher feed rate. When analyzing the deviations of the shape obtained from the comparison of nominal profile and actual surface profile, it was noted that for a_p = 10 µm and a_p = 20 µm, smaller deviations of the profile shape occurred at higher feed rates. In the grinding process a thickness of a_p = 30 µm, the deviation of shape was smaller at feedrate 200 mm/min than at feedrate 400 mm/min.

Conclusions

From the presented analysis, it is clear that the accuracy of surface mapping and its roughness depend on a number of geometric and technological parameters, especially on the speed of feed. Further studies should also examine the impact of the tilt angles of the wheel hub shaft.

REFERENCES

1. Habrat W., Wdowik R., Porzycki J., Świder J. „Określenie granicznych wartości porowatości pozornej ceramiki korundowej i cyrkonowej w stanie białym dla potrzeb obróbki ściernicami z mikrokrystalicznego korundu spiekanego”. *Mechanik*. 9 (2014): s. 143–146.
2. Kriegesmann J. “Einteilung keramischer Werkstoffe”. *Technische Keramische Loseblattausgabe*. Köln: Deutscher Wirtschaftsdienst, 2004, s. 1–20.
3. Marinescu I.D. “Handbook of Advanced Ceramics Machining”. CRC Press Taylor & Francis Group, 2007, s. 327–353.
4. Schmidt Ch. “Koordinatenschleifen dentalkeramischer Werkstoffe mit kleinen Diamantwerkzeugen”. Aachen: Shaker, 2008.
5. Rodrigues A.C., Franco de Souza R.N., Galisa O.F., Franca T.V., Bianchi E.C., Foschini C.R. “Effect of grinding parameters on surface of advanced ceramics”. *Matéria*. 21, 4 (2016): s. 1517.